

An empirical study of the naïve REINFORCE algorithm for predictive maintenance

Rajesh Siraskar^{1,3}, Satish Kumar^{1,2}, Shruti Patil^{1,2}, Arunkumar Bongale¹,
and Ketan Kotecha^{1,2}

¹Symbiosis Institute of Technology, Symbiosis International (Deemed University), Pune,
412115, Maharashtra, India

²Symbiosis Centre for Applied Artificial Intelligence, Symbiosis International (Deemed
University), Pune, 412115, Maharashtra, India

³Birlasoft Ltd., Pune, 411057, Maharashtra, India

September 28, 2023 V 2.07

Abstract

Industrial systems are highly complex and dynamic electro-mechanical systems. Reinforcement Learning (RL) offers an autonomous learning framework to generate optimal predictive maintenance (PdM) policies for such systems. RL algorithms are highly sensitive to hyperparameter tuning, and this is where Automated Machine Learning (AutoML) can offer industrial practitioners a platform, encouraging application of RL to their problems. AutoML applied to the combined fields of predictive maintenance and RL, has yet to be studied. This research is a small step in this direction. Aimed at industrial practitioners unfamiliar with complex RL tuning, we undertake an empirical study to appreciate the effects of *untuned* RL algorithms for generating an optimal tool replacement policy for a milling machine.

We compare a naïve implementation of REINFORCE against the policies of industry-grade implementations of three advanced algorithms, namely, Deep Q-Network (DQN), Advantage Actor-Critic (A2C), and Proximal Policy Optimization (PPO). Our broad goal was to study model performance under four scenarios: (1) simulated tool-wear data, (2) actual tool-wear data (benchmark IEEE *DataPort* PHM Society datasets), (3) univariate state with added noise levels and a random chance of break-down, and finally (4) complex multivariate state. Performance was measured by how accurately the PdM agent suggested tool replacement compared to a deterministic preventive maintenance rule (based on a tool-wear threshold). Across 15 environment variants, REINFORCE models demonstrated a tool replacement precision of 0.687 against 0.449 for A2C, 0.418 for DQN, and 0.472 for PPO.

The F1 scores were 0.609, 0.442, 0.374, and 0.345, respectively. Variability in precision and F1 was lower for REINFORCE by 0.08 and 0.016 compared to the average of the three advanced algorithms. Comparing the best *auto-selected* model, over ten rounds of training produced unusually wider gaps in performance. REINFORCE precision/F1 stood at 0.884/0.873. The best A2C, DQN, and PPO models produced 0.520/0.639, 0.651/0.740, and 0.558/0.580, respectively. While this study is a first tiny step toward AutoML for PdM using RL, our findings, surprisingly, indicate that the computationally lightweight REINFORCE performs significantly well for this particular problem.

For reproducibility – model training and testing code, data and the trained REINFORCE models have been uploaded to <https://github.com/Link>

Keywords: Predictive maintenance, milling machines, Reinforcement Learning, REINFORCE

Abbreviations

A2C	Advantage Actor-Critic	DQN	Deep Q-Network
PPO	Proximal Policy Optimization	RF	REINFORCE
SS	Single-variable state	MS	Multivariate state
TP	True positive	TN	True negative
FP	False positive	FN	False negative
RL	Reinforcement Learning	SB3	Stable-Baselines3
PdM	Predictive maintenance	PHM	The Prognostics and Health Management Society

1 Introduction

Milling machines are highly versatile, ubiquitous tools serving a variety of industries. A milling machine removes metal from the work piece by rotating and driving a cutting device into it. Abrasive forces cause tool wear, and optimal tool replacement reduces direct costs and optimizes the machines’ downtime. This is an important goal, considering that the global milling machine market is valued at USD 68.3 billion ([Future Market Insights, 2023](#)). The cutting tool experiences multiple types of wear as it cuts through metal. Tool wear depends on several factors such as the cutting speed, force applied to the tool, lubrication and materials of the work piece and cutting tool.

Reinforcement learning (RL) is an artificial intelligence technique inspired by nature. Fig. 1 ([Sutton and Barto, 2018](#)) shows the RL learning feedback loop. An actor or “agent” interacts with an environment and learns via “trial-and-error”. It acts based on stimuli or feedback received from the environment after performing a certain action. Actions that help in achieving the learning goal receive a reward while actions that do not, are punished. Repeating this loop over thousands of episodes, good actions are “reinforced”, thereby building a “policy” that is optimized for that goal. In the case of predictive maintenance for milling machines, the agent is the “planner” with a goal of learning an optimal tool replacement policy. The environment consists of sensors attached to the machine and related information such as job specifications, environment conditions etc.

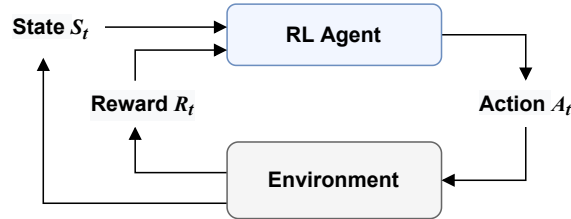


Figure 1: Reinforcement Learning

Introduced in 1992, the REINFORCE algorithm ([Williams, 1992](#)) is an early policy based RL algorithm, capable of handling both discrete and continuous observation and action spaces. In practice the REINFORCE algorithm is considered as a “weak” algorithm and superseded by several algorithms developed since. Most notably the deep-neural network version of Q-Learning, the Deep Q-Network (DQN) ([Mnih et al., 2013](#)), followed by Actor-Critic ([Mnih et al., 2016](#)) and one of the most robust modern-day algorithms, the Proximal Policy Optimization (PPO) ([Schulman et al., 2017](#)), Fig. 2.

Our study takes a fresh look at REINFORCE, an otherwise neglected algorithm since it is considered an early, naïve algorithm, comparing it against three advanced algorithms, namely, DQN, Advantage Actor-Critic (A2C), and PPO. Secondly, while most RL studies are evaluated on Open AI Gym environments, our experiments cover the predictive maintenance problem using a custom built environment. In practice the milling tool is

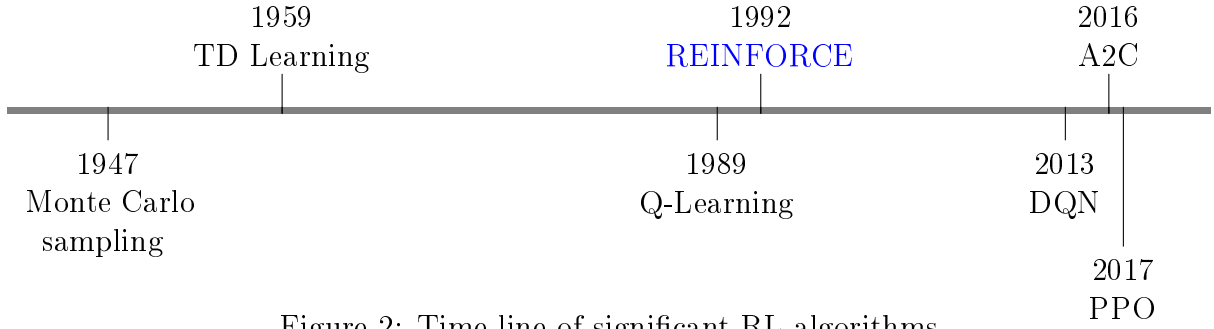


Figure 2: Time line of significant RL algorithms

replaced after a set threshold. We use this “deterministic preventive maintenance” policy as the baseline for comparing the various policies. Our systematic evaluation, based on levels of environment difficulty, different bench-mark datasets and varying noise levels allow a broader comparison of the algorithms. Finally, we conduct statistical tests to ensure a robust statistical-evidence based conclusion.

The main **contributions** of this research are:

1. Contributes to the broader goal of AutoML for PdM, using RL.
2. Research targeted toward the industrial practitioner not accustomed to complex hyper-parameter tuning of RL algorithms.
3. Design and implement an RL environment for PdM of a milling machine.
4. Rigorous evaluation of four standard, untuned , RL algorithms.
5. Use of simple performance evaluation statistical measures and plots that industrial practitioners are normally used to.

The rest of the paper is structured as follows: In the next section we survey some related work and provide the necessary technical background describing the algorithms studied in this research. Section 3 discusses implementation details of the REINFORCE algorithm and the predictive maintenance environment followed by the methodology adopted for training, testing and evaluation. Section 4 and 5 present and discuss, the results of experiments. Finally, we summarize and draw conclusions in Section 6.

2 Related work and background

2.1 Literature Review

Significant work has been conducted in the application of RL for predictive maintenance in general (Erhan et al., 2021; Panzer and Bender, 2021; Siraskar et al., 2023); however

none of them covered¹ PdM for milling machines. Similarly, automated machine learning (AutoML) for predictive maintenance was presented in only 9 research articles, with a coverage limited to supervised machine learning and therefore excluded RL.

Experimental comparison and analysis of various RL algorithms, has been limited to using standard benchmark OpenAI Gym environments. [Sandeep Varma et al. \(2022\)](#) documents experimental evaluation of four policy-gradient and actor-critic algorithms PPO, SAC, DDPG and A2C using the Pendulum, Mountain Car, Bipedal Walker, Lunar Landing and Atari 2600 game environments. [Velivela and Yarram \(2020\)](#) evaluate DQN, DoubleDQN, A2C, REINFORCE and PPO using Cartpole, Space Invaders and the Lunar Lander. [Dulac-Arnold et al. \(2020, 2021\)](#) are significant contributions toward analyzing empirical studies directed toward *real-world* challenges. They apply real-world design concepts on the Cartpole and other complex environments such as humanoids and walkers from the Real-World Reinforcement Learning (RWRL) Suite². These environments are then evaluated for multiple algorithms such as, REINFORCE, Trust Region Policy Optimization (TRPO) and Deep Deterministic Policy Gradient (DDPG).

[Dulac-Arnold et al. \(2021\)](#); [Henderson et al. \(2018\)](#) tackle RL for continuous control. [Henderson et al. \(2018\)](#) evaluate DDPG, ACKTR, TRPO and PPO on complex MuJoCo³ environments such as the HalfCheetah, Hopper, Walker and Swimmer. Similar to our research, they used the OpenAI baseline implementations of RL algorithms for the experiments and evaluation. [Ford and Ritchie \(2022\)](#) is one experimental evaluation we found based on a *real-world* application where DQN, A2C and PPO are applied for choosing the operational radio frequency (RF) mode for a multi-function RF system and go on to suggest that PPO is the best.

Our survey shows that most existing work use standard OpenAI Gym environments, which although necessary for bench-marking performance, do not provide coverage of industrial PdM. In Section 3.1 we attempt to bridge this gap by implementing a custom built environment.

2.2 Technical Background

Key concepts of RL

A task is a goal we set for our agent to learn. In our case the agent must learn to optimally predict the replacement of the tool. Frequent tool replacement increases downtime while delaying it results in inferior work piece quality. In Fig. 1 the agent interacts with the environment by performing an action ($a \in \mathcal{A}$), which then alters the state of the environment to one of many states ($s \in \mathcal{S}$). The resulting state is determined by a

¹Query: (milling OR "tool wear") AND "reinforcement learning" AND maintenance. As of: 10-Jul-2023, across IEEE Xplore™, Scopus™ and Web Of Science™

²Link to RWRL » [link](#)

³MuJoCo provides environments for studying Multi-Joint dynamics with Contact

state-transition probabilities (\mathcal{P}) since RL is founded on Markov Decision Process (MDP) theory. The new state provides a feedback via a reward ($r \in \mathcal{R}$). Higher positive rewards “reinforce” good behavior. Performing this over thousands of episodes with the objective of maximizing the total rewards R , enables the agent to develop a policy π which is essentially a mapping of the optimal action to perform given a certain state.

A **value function** computes how good a state or an action is by predicting future rewards, also known as a “return” $G_t = R_{t+1} + \gamma R_{t+2} + \dots = \sum_{k=0}^{\infty} \gamma^k R_{t+k+1}$. $\gamma \in [0, 1]$ facilitates discounting i.e. applying less weight to future rewards. Value functions can be represented by **state-value** $V_{\pi}(s)$ of a state s , as the expected return: $V_{\pi}(s) = \mathbb{E}_{\pi}[G_t | S_t = s]$; or an **action-value** function of a state-action pair as $Q_{\pi}(s, a) = \mathbb{E}_{\pi}[G_t | S_t = s, A_t = a]$.

With a brief overview of RL, we now briefly touch upon the core ideas of the four algorithms we experimented with.

Deep Q-Network (DQN)

Deep Q-Network (Mnih et al., 2013) significantly improved the earliest RL algorithm, Q-learning, by introducing neural networks to learn policies for high-dimension environments with two novel strategies to significantly stabilize learning – an “experience replay buffer” and a target network that was frozen and only periodically updated. Equation (1) shows the DQN loss function where D is the replay memory and is sampled using a uniform distribution $U(D)$, $Q(s, a; \theta)$ is the function parameterized with θ , that helps compute the Q values and θ^- represents parameters of the frozen target Q-network.

$$\mathcal{L}(\theta) = \mathbb{E}_{(s,a,r,s') \sim U(D)} \left[\left(r + \gamma \max_{a'} Q(s', a'; \theta^-) - Q(s, a; \theta) \right)^2 \right] \quad (1)$$

Advantage Actor Critic (A2C)

A2C is a variant of Asynchronous Advantage Actor Critic (A3C) (Mnih et al., 2016), and uses multiple computation workers to avoid the use of a replay buffer. A2C is a policy-gradient actor-critic algorithm. The policy-gradient family of algorithms strive to model and optimize the policy directly. Actor-critic structures consist of two networks – a critic that updates function parameters w of the value function (i.e either $Q_w(a|s)$ or $V_w(s)$); and an actor that updates the policy parameters θ for $\pi_{\theta}(a|s)$, following the direction computed by critic. Actors therefore learn the parameterized policy π_{θ} using the policy-gradient as shown in (2).

$$\nabla_{\theta} J(\pi_{\theta}) = \mathbb{E}_t \left[A_t^{\pi} \nabla_{\theta} \ln \pi_{\theta}(a_t | s_t) \right] \quad (2)$$

Where the advantage function $A_t^\pi(s_t, a_t)$ measures how good or bad the action is w.r.t. policy's average, for a particular state, using (3).

$$A_t^\pi(s_t, a_t) = Q^\pi(s_t, a_t) - V^\pi(s_t) \quad (3)$$

Proximal Policy Optimization (PPO)

Schulman et al. (2017) formulated PPO which is often considered as the most robust of the RL algorithms. PPO is a policy-gradient method based on TRPO (Trust region policy optimization) by Schulman et al. (2015), where the main idea is the use of a trust region to improve training stability by avoiding updates to parameters that vastly change the policy at a particular time step. TRPO ensures this by using a divergence constraint on the magnitude of policy update. If $r(\theta)$ (4) represents the ratio of probabilities between policies of previous and current iteration, then the objective function of TRPO is given by (5), where \hat{A} represents the estimated advantage function.

$$r(\theta) = \frac{\pi_\theta(a|s)}{\pi_{\theta_{\text{old}}}(a|s)} \quad (4)$$

$$J^{\text{TRPO}}(\theta) = \mathbb{E}[r(\theta)\hat{A}_{\theta_{\text{old}}}(s, a)] \quad (5)$$

PPO extends TRPO by additionally imposing a regional constraint. It prevents large updates by forcing the ratio $r(\theta)$ to stay within a small interval $[1 - \epsilon, 1 + \epsilon]$, around 1.0, by use of a hyper-parameter ϵ .

$$J^{\text{CLIP}}(\theta) = \mathbb{E}_t [\min(r_t(\theta)A_t^{\pi_{\theta_{\text{old}}}}, \text{clip}(r_t(\theta), 1 - \epsilon, 1 + \epsilon)A_t^{\pi_{\theta_{\text{old}}}})] \quad (6)$$

REINFORCE

The REINFORCE algorithm, invented by Williams (1992), is an early algorithm that directly learns a policy π_θ to produce action probabilities from states. Actions that cause favorable states, are positively reinforced thereby increasing their probability of occurrence. Conversely, those resulting in unfavorable states are penalized.

The objective function (7) that the agent attempts to maximize is defined as the expected return over many trajectories sampled from the policy.

$$\max_{\theta} J(\pi_\theta) = \mathbb{E}_{\tau \sim \pi_\theta} [R(\tau)] \quad (7)$$

REINFORCE uses policy gradient (8) to update the action probabilities.

$$\nabla_{\theta} J(\pi_\theta) = \mathbb{E}_t [R_t(\tau) \nabla_{\theta} \ln \pi_\theta(a_t|s_t)] \quad (8)$$

3 Methodology

3.1 Implementation details

RL requires an environment to function. In this section we describe the custom milling environment we built, which allows our agent to learn a policy for tool replacement. Fig. 3 shows the stepped approach used to generate the fifteen environments, of varying complexity. We next describe each variant starting with the simulation-based, followed by real-data based; describing their sub-variants along the way.

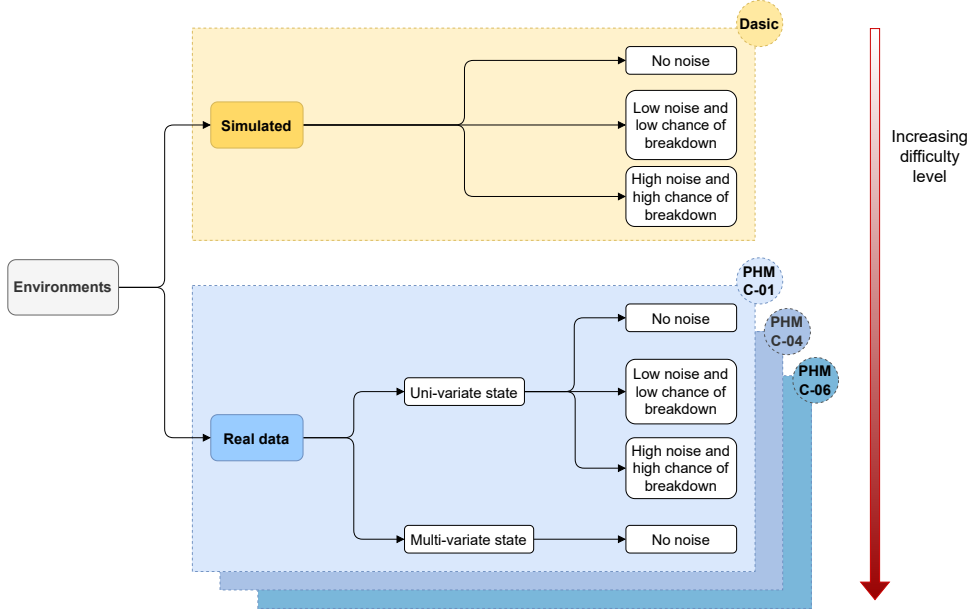


Figure 3: The fifteen different environments used for evaluation.

Simulating tool wear

Dašić (2006) provides a parameterized power-exponential function for modeling tool wear (9), where VB represents the flank wear in mm.

$$VB = a \cdot t^{b_1} \cdot e^{b_2 \cdot t} \Big|_{t=t_0}^{t=t_1} \quad (9)$$

We used the parameter values provided in the paper $a = 0.08257$, $b_1 = 0.3342$ and $b_2 = 0.03147$ to simulate 120 data points. Fig. 4a shows the tool wear simulated using (9), with the red dotted-line indicating the wear threshold beyond which tool is replaced. This provided the mechanism to simulate the basic variant of tool-wear based **univariate state**. We then added two further levels of increased complexity using noise and a chance of breakdown, giving us three distinct environments.

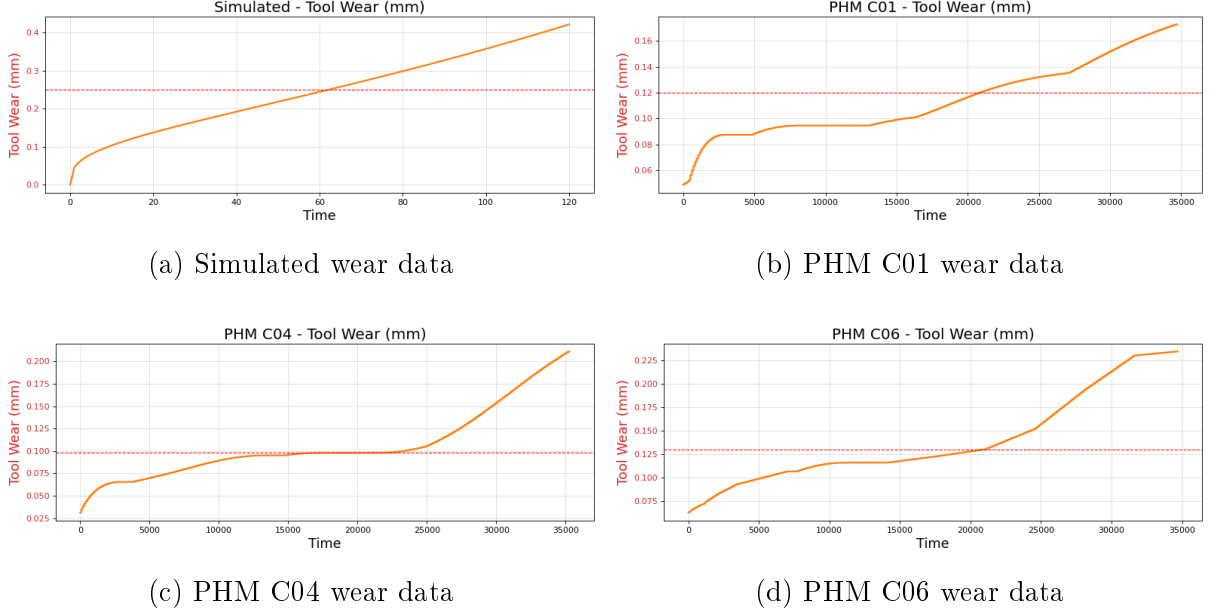


Figure 4: Tool wear data. Red dotted line indicates the wear threshold beyond which tool is replaced.

Actual tool wear data

The *IEEEDataPort* hosts the “2010 PHM Society” tool-wear data obtained from a high-speed CNC milling machine, (Li, 2021). C01, C04 and C06 datasets are suggested as benchmarks to be used for machine learning research and were the ones we used⁴. The data is from seven sensors – dynamometer measuring forces in X, Y and Z dimensions, measured in N ; accelerometer measuring vibration in X, Y and Z dimensions, measured in g and finally acoustic emission data as AE-RMS, in V . A separate file contains tool wear data in mm . Figures 4b, 4c and 4d show the tool wear for the three datasets. We use real data to create two state designs, an univariate state consisting of only the tool wear and a **multivariate** state designed using all the additional seven sensor values. Just as we did for the simulated case, the complexity of the univariate state is increased using two levels of noise and break-down parameters. The multivariate state is complex in itself, Fig. 5, and we use the natural (without noise) form.

In practice, state variables are often normalized to improve stability and convergence. Both the simulated and real data was normalized using min-max scaling such that the tool wear and other state features, $x \in [0, 1] \subset \mathbb{R}$. We will see next how this allows adding white noise of similar magnitudes across different PHM datasets.

⁴In the article, we often refer to these datasets as “PHM-” data.

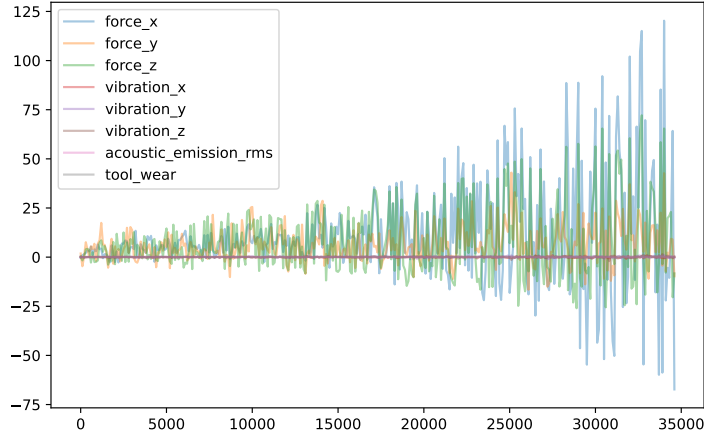


Figure 5: PHM C06: multivariate data

Adding noise and chance of break-down

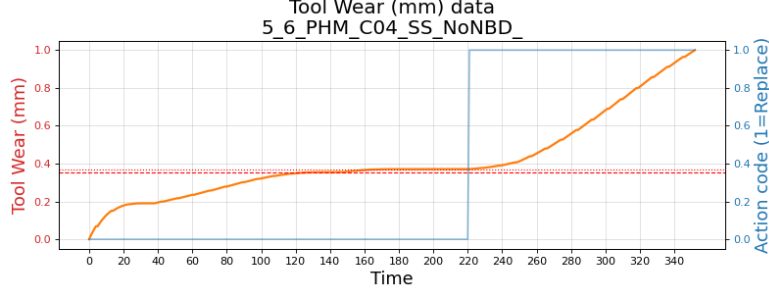
Fig. (6) shows the effect of adding two levels of noise. “Low noise” is obtained by adding Gaussian noise with an order of magnitude of -3 i.e. $[0.0, 0.001]$ and “high noise” is of order -2 i.e. between $[0.0, 0.01]$. Since the tool wear is less than 0.24 mm, this adds significant perturbations as seen in Fig. (6b) and (6c). The noise affects the tool replacement decision (solid blue line) around the replacement threshold (dotted red line). The *human* preventive maintenance policy replaces the tool if the wear exceeds the threshold and this decision boundary oscillates due to the noise. One can see that in the case of no noise (Fig. 6a), the decision boundary is clean.

Break down occurs due to excessive tool use and can often occur randomly. In conjunction with Gaussian noise this complexity is added for the univariate state based environments. For the low-noise variant we add a low 5% chance of break down and for the high noise variant we add a higher chance of 10%. The “milling” episode is terminated if a probability, sampled from a uniform distribution is less than this “chance” threshold.

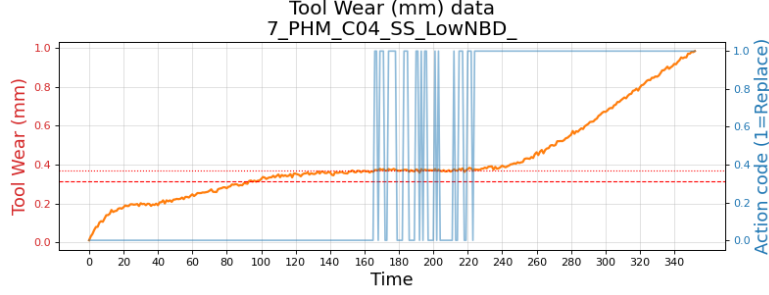
Table 1 summarizes the 15 environment variants and their three logical groups: (1) Simulated 1-3 (2) Real data – simple univariate environment (4-12) and Real data – complex multivariate (13-15).

Tool wear as a Markov Decision Processes (MDP)

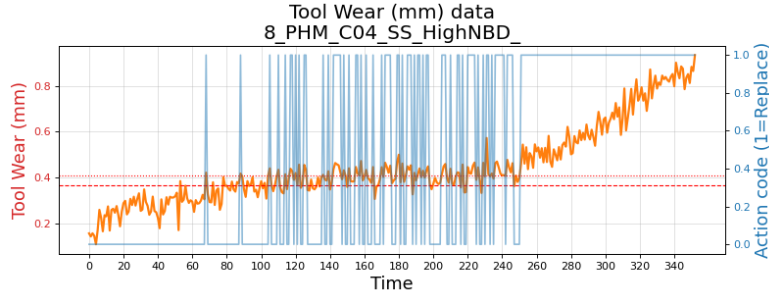
Formulating our problem to be solved by RL requires us to assume that the wear process satisfies the Markov property – which implies that the transition of tool wear to another state is dependent only on the current state and not on any previous states. MDPs are defined by the tuple $\langle \mathcal{S}, \mathcal{A}, \mathcal{P}, \mathcal{R}, \gamma \rangle$. We will define the elements of state space \mathcal{S} , action space \mathcal{A} and reward function \mathcal{R} , next.



(a) No noise



(b) Low noise



(c) High noise

Figure 6: PHM C04 tool wear data (normalized) and the effect of noise. Blue line is the replacement action decision.

State and environment elements

There are two basic state definitions across the 15 environment variants, the “simple univariate” and the “complex multivariate”.

The elements of simple univariate state vector are $S_t = [w_t]$, where w_t is the current tool wear. As part of the environment other elements that are sensed by the agent are $[W_\tau, N_f, P_{bd}]$, where W_τ is the wear threshold, N_f is the noise factor and is one of $[0, 1e-3, 1e-2]$, P_{bd} is the chance of tool breakdown and is one of $[0, 0.05, 0.10]$. The complex multivariate state $S_t = [f_x, f_y, f_z, v_x, v_y, v_z, ae_{rms}, w_t]$ where, as mentioned in Section 3.1, (f_x, f_y, f_z) represents the force along the 3 axes, similarly v represents the vibration, ae_{rms} the acoustic emission.

	Environment variant	Noise factor	Breakdown chance
Simulated			
1	Simulated - No noise	None	None
2	Simulated - Low noise	1e-3	0.05
3	Simulated - High noise	1e-2	0.10
Real data – simple univariate			
4	PHM C01 SS (simple, univariate) - No noise	None	None
5	PHM C01 SS (simple, univariate) - Low noise	1e-3	0.05
6	PHM C01 SS (simple, univariate) - High noise	1e-2	0.10
7	PHM C04 SS (simple, univariate) - No noise	None	None
8	PHM C04 SS (simple, univariate) - Low noise	1e-3	0.05
9	PHM C04 SS (simple, univariate) - High noise	1e-2	0.10
10	PHM C06 SS (simple, univariate) - No noise	None	None
11	PHM C06 SS (simple, univariate) - Low noise	1e-3	0.05
12	PHM C06 SS (simple, univariate) - High noise	1e-2	0.10
Real data – complex multivariate			
13	PHM C01 MS (complex, multivariate) - No noise	None	None
14	PHM C04 MS (complex, multivariate) - No noise	None	None
15	PHM C06 MS (complex, multivariate) - No noise	None	None

Table 1: List of the fifteen environments and their categorization

Actions

The action space is binary, $\mathcal{A} \in [0, 1]$, where 0(**CONTINUE**) represents continuation of milling operation and 1(**REPLACE_TOOL**) represents the action of replacing the tool.

Environment feedback

“Feedback” generated by the action an agent takes, is the central mechanism by which agents learn. This is implemented via the `step()` function in the environment code and is outlined in Algorithm 1. At every time step an action A_t is taken and the resulting state is evaluated for terminating conditions or assigning a reward and continuing.

Reward function

$$R_t = \begin{cases} +R_1 \times t, & \text{if } w_t < W_\tau \\ -R_2 \times t, & \text{if } w_t \geq W_\tau \\ += -R_3, & \text{if ACTION} = \text{REPLACE_TOOL} \end{cases} \quad (10)$$

In the reward function (10) there are three distinct phases where a reward (or penalty) is offered as feedback. R_1 , R_2 and R_3 are constants that determine the magnitude of reward. When the current state of wear w_t is less than the threshold W_τ we have a desirable condition, and we award the agent a positive reward. The formulation (10) allows a higher reward to be collected the closer it is to threshold so as to maximize tool usage, but not allowing it to cross it. If it does, the agent is penalized (negative reward) by a magnitude of R_2 , and once again the farther away it is from the threshold i.e. a highly deteriorated tool the larger the penalty. To avoid this “bad” state, the agent must learn to replace the tool; represented by the third condition. Tool replacement implies a direct cost (that of the tool) and a much higher and significant downtime “cost”. To ensure the agent does not learn to replace unnecessarily, we “penalize” it. It is important to note that the last condition in (10) is an “incremental addition”, the first two conditions are mutually exclusive and evaluated first, followed by the last condition which is incrementally added on whatever reward is collected in the previous condition. The agent then tries to balance these three conditions, such that it maximizes its total return, over time.

Of the final two elements of the MDP quintuple \mathcal{P} represents the probability transition matrix and is usually not known and we will therefore use *model-free* RL techniques to learn that from “experiences”; γ enables the agent to learn long-term impact of its actions i.e. what is the long term impact of replacing the tool now or that of delaying the replacement, γ is set to 0.99 to facilitate this farsightedness.

Network architecture and basic hyper-parameters

Stable-Baselines3 (SB3) [Raffin et al. \(2021\)](#) provides robust open source implementations of many RL algorithms. As of 10-Jul-2023, 13 algorithms have been implemented ([SB3-Algorithms, 2022](#)) however REINFORCE has *not* been implemented. For this research we use the *default* SB3 implementations of DQN, A2C and PPO and compare its performance to a custom implementation of the REINFORCE algorithm using a very simple network architecture. Table 2 shows a comparison of the architecture and the basic common hyper-parameters. The REINFORCE uses a *single* internal layer of 64 units. The default architecture for all three SB3 algorithms (A2C/DQN/PPO) consists of *two* fully connected layers with 64 units per layer ([SB3-Default Network Architecture, 2022](#)). While REINFORCE used ReLU (rectified linear unit) as the activation function, the other three

Algorithm 1 Agent class `step()` method – Reward handling mechanism

1: **procedure** STEP CLASS METHOD: REWARD HANDLING

Class attributes: Wear-threshold W_τ , reward accumulated so far $Reward$, reward function parameters $R1$, $R2$ and $R3$, random chance of breakdown P_{bd} , tool replacements made so far $tool_replacements$, maximum allowable operations T

Input: Current length of episode t , current tool-wear w_t , current policy action A_t , current index of training data $data_index$

2: **Initialize** p from uniform probability distribution

3: **if** $t \geq T$ **then:**

4: \triangleright Termination based on length of episode.

5: $Terminate \leftarrow True$

6: $Reward \leftarrow 0.0$

7: $data_index \leftarrow 0$ \triangleright Reset the training data-frame index to the beginning.

8: **else if** $w_t > W_\tau$ **and** $p < P_{bd}$ **then:**

9: \triangleright Termination based on chance of breakdown.

10: $Terminate \leftarrow True$

11: $Reward \leftarrow 0.0$

12: $data_index \leftarrow 0$

13: **else**

14: $Terminate \leftarrow False$

15: **if** $w_t < W_\tau$ **then:**

16: \triangleright Healthy tool

17: $Reward \leftarrow Reward + t \cdot R1$

18: **else**

19: \triangleright Tool deteriorating

20: $Reward \leftarrow Reward - t \cdot R2$

21: **if** A_t is `REPLACE_TOOL` **then:**

22: \triangleright Tool is replaced

23: $Reward \leftarrow Reward - R3$

24: $data_index \leftarrow 0$ \triangleright Tool replaced, therefore roll back tool life

25: Increment $tool_replacements$

algorithms used hyperbolic tangent (Tanh). Finally, REINFORCE's learning-rate is also much larger.

	A2C	DQN	PPO	REINFORCE
Network architecture	input dim x [64 Tanh x 64 Tanh] x output dim	input dim x [64 Tanh x 64 Tanh] x output dim	input dim x [64 Tanh x 64 Tanh] x output dim	input dim x [64 ReLU] x output dim
Layers	2	2	2	1
Units	64 x 64	64 x 64	64 x 64	64
Activation	Tanh, Tanh	Tanh, Tanh	Tanh, Tanh	ReLU
Optimizer	RMSprop	Adam	Adam	Adam
Learning rate	0.0007	0.0001	0.0003	0.01
Gamma	0.99	0.99	0.99	0.99

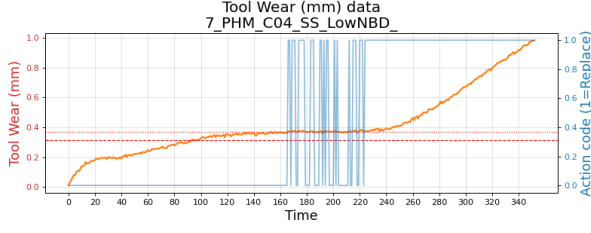
Table 2: Comparing the network architecture and basic hyper-parameters across algorithms

3.2 Training

The training strategy must ensure a uniform comparison of the algorithms. We maintained the exact *same* environment variant, wear dataset, noise parameter, probability of breakdown parameter, and the three reward function parameters; across all four algorithms during a single training round. As the wear data is time-series data, the training and test sets are created by systematic sampling. Simulated data and real tool wear data (PHM) was randomly sampled at a certain frequency and down sampled into training and test sets.

The REINFORCE was trained for 800 episodes for the simulated and PHM univariate variants, for all three noise and breakdown levels (none, low and high) – Table 1 items 1-12. For the PHM multivariate variant, Table 1 items 13-15, REINFORCE was trained for 1000 episodes. SB3 algorithms were trained for 10,000 episodes for all variants. We ran ten rounds of training, tested each generated model and averaged results over the 10 rounds. Testing is explained in the next section while results are presented in Section 4.

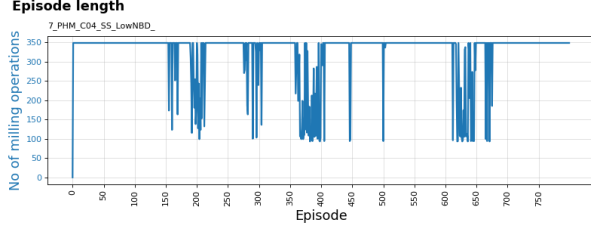
Fig. 7 shows the training plots for the algorithm of our interest – REINFORCE. It displays how the wear plot looked for C04 with low noise and low chance of breakdown settings. The average rewards increase over the course of 800 episodes (Fig. 7b). The episode length (Fig. 7c) demonstrates the complexity introduced by random breakdown (which abruptly terminates the episode). It is the tool replacement policy that is of interest to the industrial practitioner – Fig. 7d shows that it decreases to optimal levels as the agent learns over time. Similarly, Fig. 8 demonstrates the training for the PHM



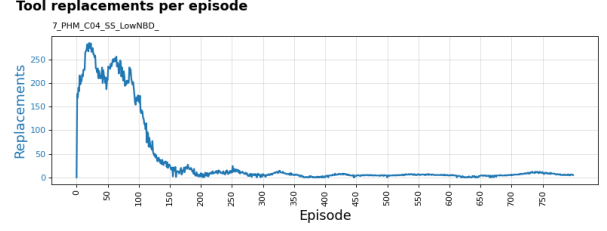
(a) PHM C04 wear data



(b) Average rewards per episode



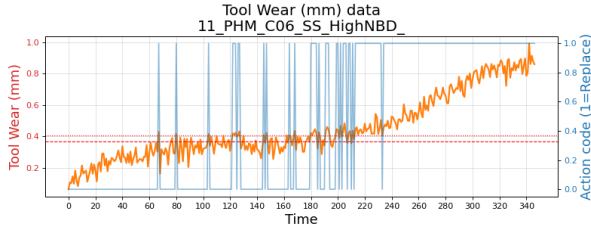
(c) Episode length completed per episode



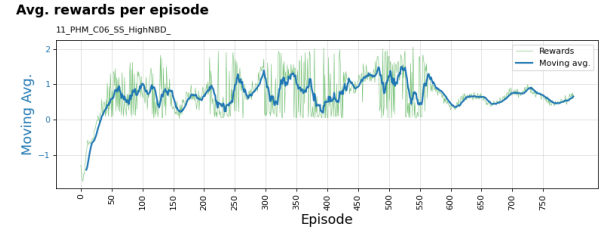
(d) Tool replacements per episode

Figure 7: Training plots of REINFORCE. Dataset: PHM-C04. Variant: Univariate state, low-noise and low chance of breakdown.

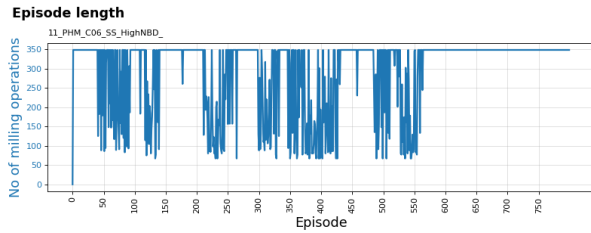
C06 dataset affected by high noise and higher breakdown probability. Finally, for the more complex multivariate state variant, the training plots are as seen in Fig. 9; as we do not introduce noise or breakdown here, the episodes are always completed (Fig. 9c).



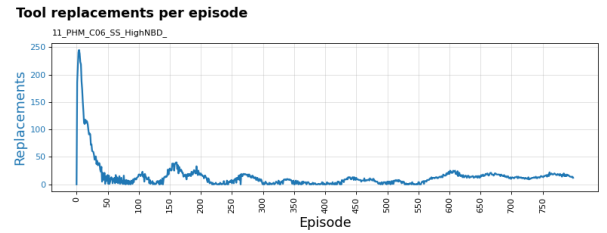
(a) PHM C06 wear data



(b) Average rewards per episode

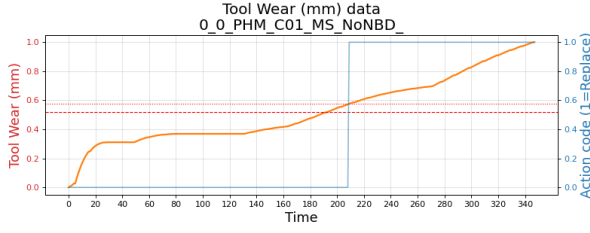


(c) Episode length completed per episode

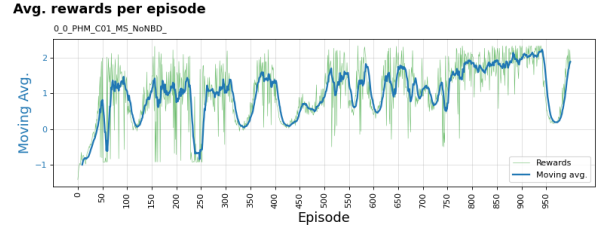


(d) Tool replacements per episode

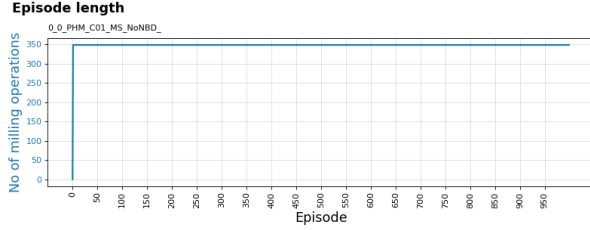
Figure 8: Training plots of REINFORCE. Dataset: PHM-C06. Variant: Univariate state, high-noise and high chance of breakdown.



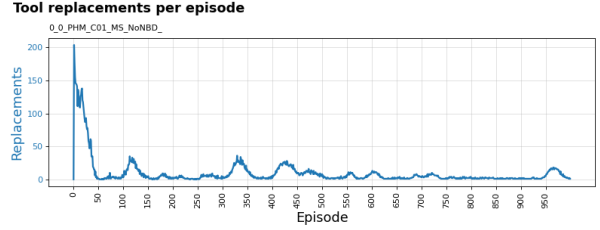
(a) PHM C01 wear data



(b) Average rewards per episode



(c) Episode length completed per episode



(d) Tool replacements per episode

Figure 9: Training plots of REINFORCE. Dataset: PHM-C01. Variant: Multivariate state, No noise or breakdown.

3.3 Testing and performance evaluation

Testing was performed with data separate from the training data. 10 rounds of testing are performed, with a *new* set of 40 test cases randomly sampled and frozen across all four algorithms, during each round.

Evaluation metrics

The human decision is based on “preventive maintenance” – replace the tool against a predefined wear threshold. In our data a tool replacement is represented as 1 and a normal operation as 0. We applied classification metrics to evaluate the RL agent decisions of tool replacement. It is worth noting that while we have selected an arbitrary wear threshold as this serves our purpose for algorithm comparison; in reality the threshold is based on several factors like materials of tool and work-piece, the duration of continuous operation, ambient conditions, “cost” of production downtime etc. Threshold could therefore vary significantly from one case to another.

		Human decision	
		Replace tool	Continue milling
Agent decision	Replace tool	TP	FP
	Continue milling	FN	TN

Figure 10: Confusion matrix: Human versus Agent decisions

Classification metrics are based on the confusion matrix shown in Fig. 10. TP represents true positive cases, where both the agent and human agree on replacing the tool. False positive FP cases denote the agent falsely suggesting replacements, while false negatives FN are cases where continuation of milling is suggested, when in fact a tool replacement would have helped. Precision (Pr), Recall (Rc) and F1-score metrics can then be computed as shown in (11).

$$\text{Pr} = \frac{TP}{TP + FP}, \quad \text{Rc} = \frac{TP}{TP + FN}, \quad \text{F1-score} = 2 \times \frac{\text{Pr} \times \text{Rc}}{(\text{Pr} + \text{Rc})} \quad (11)$$

Tool replacement precision: Timely replacements, TP , ensure work piece quality. While we desire high TP s, we do not want *unnecessary* replacements which would otherwise and reduce costly production downtime, we therefore want lower FP s. The precision metric is therefore an ideal performance metric.

While we prefer a high precision, we do want a reasonably high recall i.e. do not want to miss replacement opportunities (low FN s). The F1-score (true harmonic mean of precision and recall) gives us a *balanced* measure. Equation (12) provides a *weighted* mechanism to provide a higher F-score for higher precision, by setting $\beta < 1.0$. For our evaluation we set β to 0.5.

$$F_{\beta} = (1 + \beta^2) \cdot \frac{\text{Pr} \times \text{Rc}}{(\beta^2 \cdot \text{Pr} + \text{Rc})} \quad (12)$$

4 Results

We present the summarized results in this section accompanied by commentary referring to detailed results made available in Appendix A. Since there are several tables and figures, for reference, we created a cross-linked Table 3. Generally, blue text is used in tables to highlight prominent values. Summary performance and $F_{\beta 0.5}$ plots accompany tables to assist in visualizing the comparative performance. The $F_{\beta 0.5}$ plots show *individual* performance over ten rounds of training-validation and help infer training stability. Similar plots for precision, recall and F1 have been relegated to Appendix A.

4.1 Overall performance

At an aggregated level, Table 4 along with Fig. 11, show that the REINFORCE scores better than the other algorithms, on all four metrics. Tool replacement precision at 0.687, is highest of the four algorithms and better by 0.215 in absolute terms when compared to the next best, PPO. The standard deviation for precision is the lowest at 0.059. On recall, F1 and $F_{\beta 0.5}$, REINFORCE is better by 0.125, 0.168 and 0.195 compared to the next best.

Item	Reference
Summary Results	
1 Overall summary – All 15 environments, averaged over 10 rounds –"– $F_{\beta}0.5$ behavior plot over 10 rounds	Table 4, Fig. 11 Fig. 12
2 Simple univariate state – Simulated data, 3 variants (3 noise settings), averaged over 10 rounds –"– $F_{\beta}0.5$ behavior plot over 10 rounds	Table 5, Fig. 13 Fig. 14
3 Simple univariate state – Real data, 9 variants (3 datasets \times 3 noise settings), averaged over 10 rounds –"– $F_{\beta}0.5$ behavior plot over 10 rounds	Table 6, Fig. 15 Fig. 16
4 Complex multivariate state – Real data, 3 variants (3 datasets), averaged over 10 rounds –"– $F_{\beta}0.5$ behavior plot over 10 rounds	Table 7, Fig. 17 Fig. 18
Super Models	
5 Super Models – Best model, <i>averaged</i> over all 15 environments Super Models – Best model, <i>details</i> of all 15 environments	Table 8 Fig. 19 Appendix A - Table 11
Hypothesis tests and Training time results	
6 Hypothesis tests – p-value and t-statistic of REINFORCE versus other algorithms	Table 9
7 Training time – Averaged over 10 rounds and all 15 variants	Fig. 20
Detailed Results - Appendix A	
8 Complete detailed results – All 15 environments, averaged over 10 rounds	Appendix A - Table 10
9 Stability behavior plots over 10 rounds, Precision, Recall and F1 Overall (all variants) Simulated state Simple univariate state Complex multivariate state	Apx. A - Fig. 21 Apx. A - Fig. 22 Apx. A - Fig. 23 Apx. A - Fig. 24

Table 3: Reference table for results.

These metrics were averaged over 10 rounds of training followed by validation. We visualize the behavior of our primary metric $F_{\beta}0.5$, *individually* across the ten rounds in Fig. 12. The blue line floating above the rest of the algorithms, for all metrics, is that of REINFORCE and appears fairly stable across the ten rounds. The error-bars are also

	Precision		Recall		F1-score		$F_{\beta 0.5}$	
	Mean	SD	Mean	SD	Mean	SD	Mean	SD
A2C	0.449	0.088	0.480	0.084	0.442	0.070	0.436	0.071
DQN	0.418	0.185	0.504	0.032	0.374	0.035	0.348	0.058
PPO	0.472	0.144	0.316	0.087	0.345	0.091	0.393	0.105
REINFORCE	0.687	0.059	0.629	0.051	0.609	0.050	0.631	0.052

Table 4: Model performance summary - averaged over all environments.

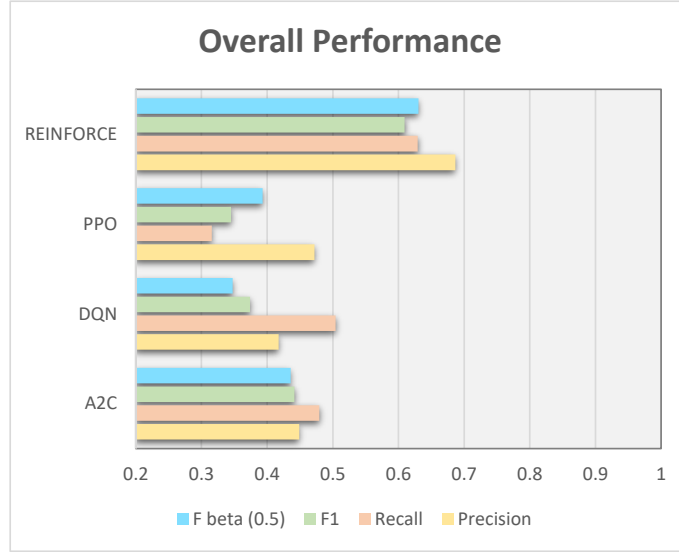


Figure 11: Overall model performance summary

pretty small, indicating lower uncertainty. We notice that the other three algorithms are all centered closely around, 0.4.

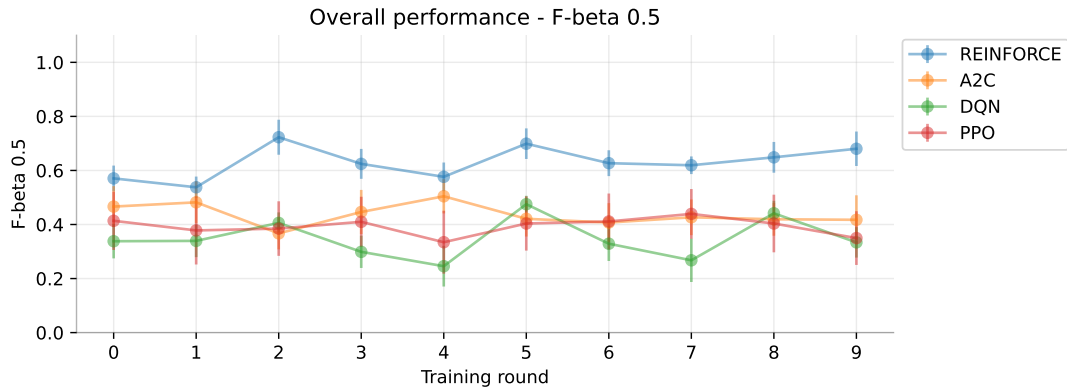


Figure 12: Overall performance comparison of the $F_{\beta 0.5}$ metric, over 10 rounds of training and testing.

We now dig into the detailed metrics Appendix A - Table 10 to better understand the aggregated summary. The largest values are typeset in blue. And a quick visual glance

shows the dominance of REINFORCE. The notable exceptions are the PHM C01 single-state and no-noise variant where A2C and DQN do better, followed by PHM C01 and PHM C06 univariate-state, low-noise variants where A2C performs better in every aspect and finally the PHM C04 and C06 multivariate variants where A2C again performs better on recall and which in turns drives the F1 score up. Barring these three complete cases and two cases where A2C recall was better, the REINFORCE performs best in ten variants and in two cases its precision, and therefore $F_{\beta}0.5$, is highest. This corroborates the overall performance observed in Table 4. Finally, Fig. 21 shows that the stability across multiple rounds is evident for other metrics as well.

4.2 Simulated environment

	Precision		Recall		F1-score		$F_{\beta}0.5$	
	Mean	SD	Mean	SD	Mean	SD	Mean	SD
A2C	0.416	0.120	0.385	0.073	0.363	0.072	0.373	0.082
DQN	0.432	0.184	0.510	0.031	0.374	0.034	0.351	0.056
PPO	0.500	0.178	0.215	0.081	0.285	0.099	0.370	0.122
REINFORCE	0.806	0.040	0.915	0.038	0.841	0.035	0.816	0.037

Table 5: Simulated environments - model performance summary.

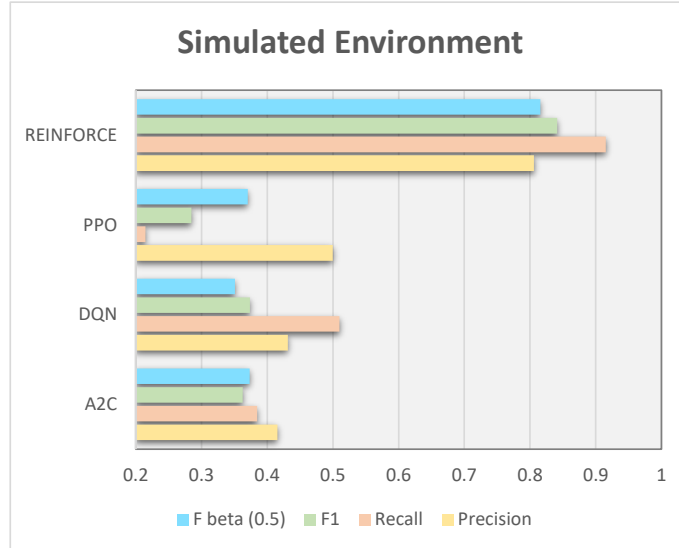


Figure 13: Simulated environments - model performance summary.

The simulated tool-wear environment is relatively the simplest for the agent to learn, even with added noise and chance of breakdown. Table 5 shows the averaged performance over the three variants. The REINFORCE performs the best and in absolute terms it

is better than the next best advanced algorithm by very high margins: precision by 0.306, recall by 0.405, F1 by 0.468 and $F_{\beta}0.5$ by 0.442, with standard deviation lower or marginally higher than others. $F_{\beta}0.5$ plot Fig. 14 shows an exceptionally consistent performance, over all ten trained models, vis-a-vis the other algorithms. Plot Fig. 22 shows DQN fluctuating heavily, occasionally showing recalls at the REINFORCE levels (rounds 2 and 8).

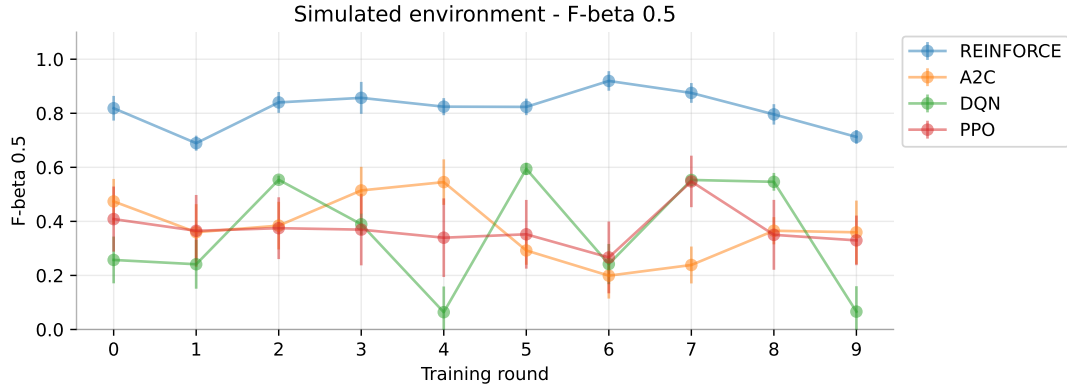


Figure 14: Simulated environments - $F_{\beta}0.5$ metric, over 10 rounds of training and testing.

4.3 Real data - simple univariate environment

	Precision		Recall		F1-score		$F_{\beta}0.5$	
	Mean	SD	Mean	SD	Mean	SD	Mean	SD
A2C	0.447	0.077	0.477	0.091	0.452	0.072	0.446	0.070
DQN	0.419	0.179	0.507	0.032	0.379	0.036	0.352	0.057
PPO	0.450	0.146	0.314	0.082	0.333	0.087	0.374	0.102
REINFORCE	0.605	0.046	0.603	0.046	0.570	0.041	0.576	0.040

Table 6: Model performance summary - averaged over PHM-2010 environments with simple single-variable environment.

Real data offers a more challenging environment. Despite this, in Table 6, we notice that REINFORCE still performs better than the other algorithms. The margins are understandably lower: precision by 0.155, recall by 0.097, F1 by 0.117 and $F_{\beta}0.5$ by 0.130. For these variants the $F_{\beta}0.5$ plot Fig. 14 shows a considerably higher performance over 9 of the 10 training rounds. Behavior of the other metrics is seen in Fig. 23. While the REINFORCE precision is higher for most rounds, the recall seems to be occasionally surpassed slightly by DQN’s (1, 8 and 9) and by a larger margin once (5).

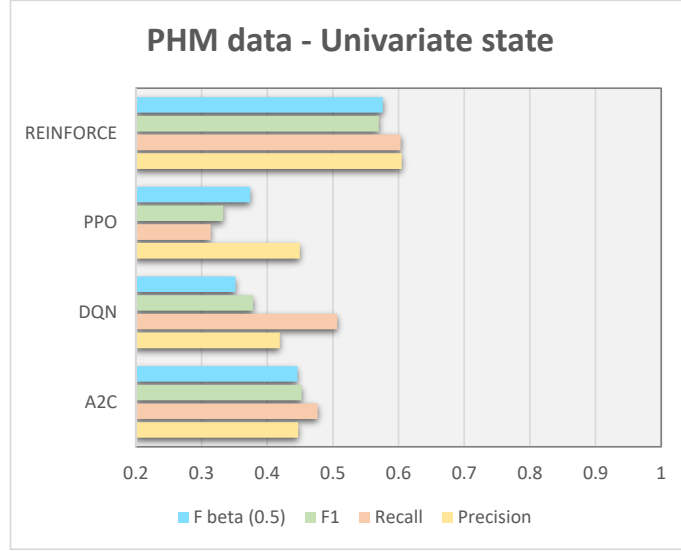


Figure 15: PHM real data - Model performance summary for the simple single-variable environment.

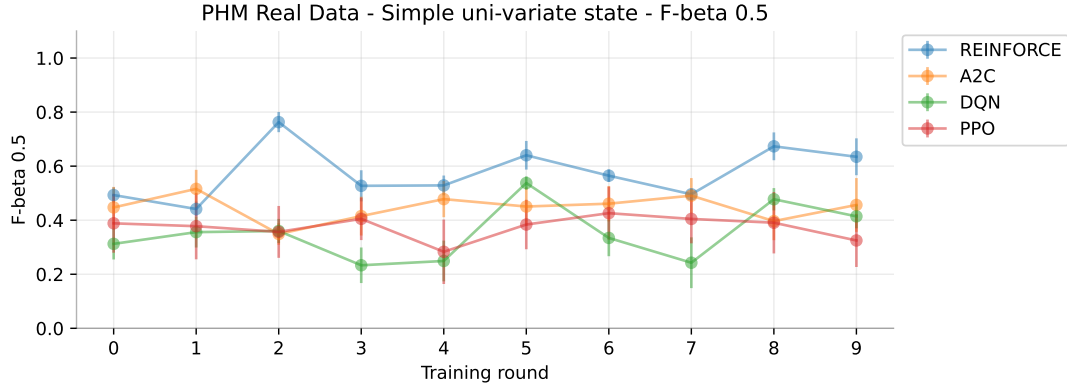


Figure 16: Univariate simple state environments - $F_{\beta 0.5}$ metric, over 10 rounds of training and testing.

4.4 Real data - complex multivariate state

	Precision		Recall		F1-score		$F_{\beta 0.5}$	
	Mean	SD	Mean	SD	Mean	SD	Mean	SD
A2C	0.487	0.086	0.582	0.075	0.488	0.063	0.467	0.065
DQN	0.399	0.204	0.491	0.032	0.361	0.035	0.332	0.060
PPO	0.512	0.107	0.422	0.107	0.441	0.096	0.472	0.096
REINFORCE	0.813	0.119	0.421	0.079	0.495	0.090	0.609	0.101

Table 7: Model performance summary - averaged over PHM-2010 environments with complex multivariate environment.

This environment offers the highest difficulty. We use real data, from *multiple* sensors.

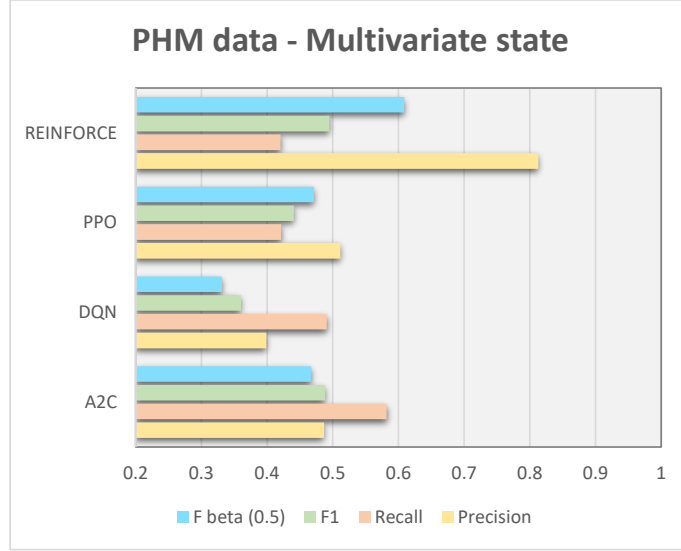


Figure 17: PHM real data - Model performance summary for the complex multivariate environment.

As with other scenarios, we used untuned, default settings of all algorithms. In Table 6, we see that the REINFORCE has the poorest recall at 0.421, however it demonstrates a surprisingly high tool replacement precision at 0.813, which drives the F1 and $F_{\beta}0.5$ to the top of the table. $F_{\beta}0.5$ performance is reflected in the Fig. 14; where it remains high for most rounds. The plot, in Appendix A, Fig. 24 shows REINFORCE’s high precision behavior. However, it is important to note that the error-bars are occasionally larger (rounds 0, 2, 4 and 6). The recall seemed higher at some points but lower half the times. The F1 appears to be in range of all the other algorithms.

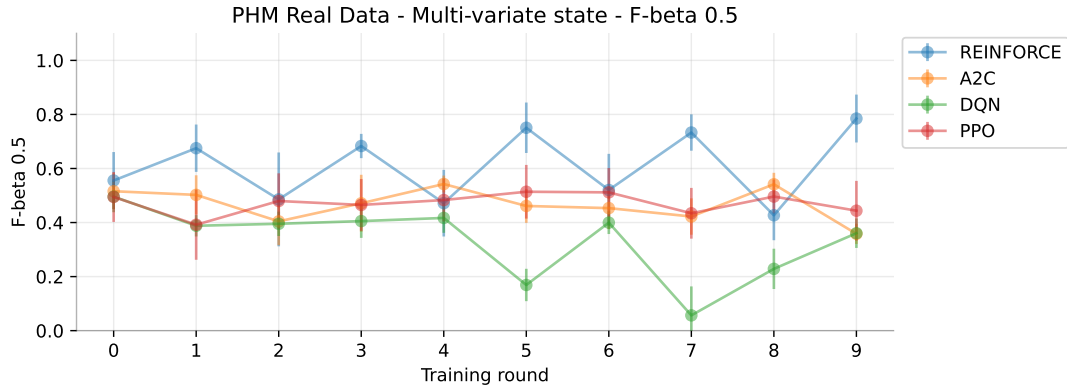


Figure 18: Multivariate complex state environments - $F_{\beta}0.5$ metric, over 10 rounds of training and testing.

4.5 Super models

Finally, we look at performance of “select” models. Logically, one would choose the best model from a set of 10 trained models. Selecting models that produce the highest F1

with a minimum criteria for precision and recall allowed us to evaluate performance of “super-models” for each algorithm. In Table 11, the REINFORCE performs better than the other three algorithms by a huge margin, for 14 of the 15 variants. For the PHM C06, univariate environment, the DQN performs the best, with extremely high metrics throughout and an F1 of 0.969 to 0.831 of REINFORCE.

As an overall average performance, Table 8 demonstrates the remarkable performance of the simple REINFORCE algorithm. It does show a lower recall when compared to the DQN, however it is a much more *balanced* model on an overall basis.

	Precision		Recall		F1-score		$F_{\beta}0.5$	
	Mean	SD	Mean	SD	Mean	SD	Mean	SD
A2C	0.520	0.031	0.859	0.053	0.639	0.036	0.560	0.032
DQN	0.651	0.022	0.937	0.031	0.740	0.022	0.678	0.021
PPO	0.558	0.076	0.643	0.097	0.580	0.079	0.562	0.075
REINFORCE	0.884	0.042	0.884	0.042	0.873	0.034	0.876	0.036

Table 8: Super models: Best of 10 rounds; performance averaged over all 15 environments.

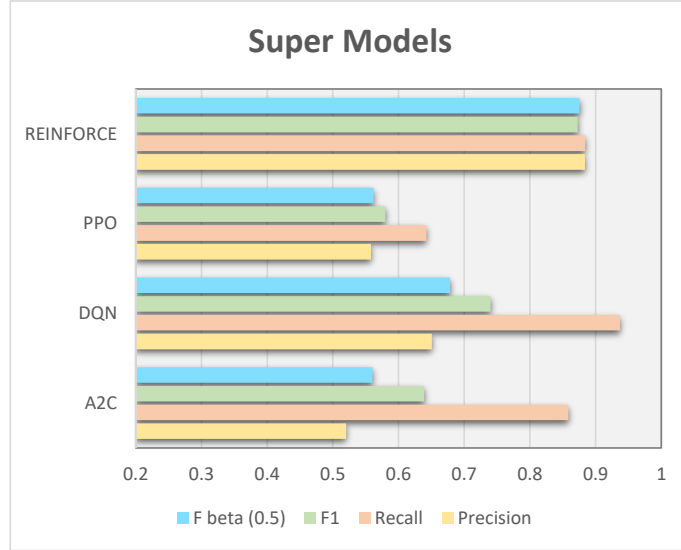


Figure 19: Super models: Best of 10 rounds; performance averaged over all 15 environments.

4.6 Hypothesis testing

We undertake a statistical analysis of the results, postulated by the hypothesis (13). Table 9 shows the result of a one-sided, two-sample t-test, conducted for a significance

level $\alpha = 0.05$. Sample size of the test are mentioned against each category⁵.

$$\left. \begin{array}{l} H_0 : \mu_{RF} - \mu_{AA} = 0, \\ H_a : \mu_{RF} - \mu_{AA} > 0, \end{array} \right\} \quad \forall AA \in [A2C, DQN, PPO] \quad (13)$$

We see that the p-values are extremely low and test statistic positive, for all cases except for the *recall* in the PHM multivariate state case. We can thus reject H_0 .

Metric	p Value			t Statistic		
	$\text{RF} \underset{H_0}{\overset{H_a}{\geq}} \text{A2C}$	$\text{RF} \underset{H_0}{\overset{H_a}{\geq}} \text{DQN}$	$\text{RF} \underset{H_0}{\overset{H_a}{\geq}} \text{PPO}$	$\text{RF} \underset{H_0}{\overset{H_a}{\geq}} \text{A2C}$	$\text{RF} \underset{H_0}{\overset{H_a}{\geq}} \text{DQN}$	$\text{RF} \underset{H_0}{\overset{H_a}{\geq}} \text{PPO}$
Overall (1500 samples)						
Precision	4.31E-126	2.17E-109	2.81E-106	25.071	23.170	22.804
Recall	4.20E-35	3.37E-16	4.36E-150	12.522	8.206	27.650
F1 score	1.99E-64	1.46E-88	5.29E-155	17.364	20.634	28.160
Simulated environment (300 samples)						
Precision	3.20E-98	1.69E-63	2.65E-81	25.611	19.032	22.427
Recall	8.12E-104	2.56E-41	1.57E-264	26.665	14.558	62.541
F1 score	9.60E-134	8.56E-99	2.96E-242	32.402	25.719	56.575
PHM Real data - Simple univariate state (900 samples)						
Precision	2.27E-32	7.29E-31	9.95E-31	12.082	11.770	11.742
Recall	1.27E-16	1.55E-06	8.19E-71	8.357	4.821	18.607
F1 score	1.94E-19	4.67E-34	2.19E-67	9.121	12.423	18.098
PHM Real data - Complex multivariate state (300 samples)						
Precision	1.64E-60	3.34E-54	7.88E-59	18.451	17.207	18.122
Recall	2.69E-10	2.69E-02	9.68E-01	-6.425	-2.219	-0.041
F1 score	7.27E-01	1.44E-08	1.35E-03	0.349	5.748	3.220

Table 9: Statistical test: One-sided two-sample t-tests. $H_0 : \mu_{RF} - \mu_{AA} = 0$; $H_a : \mu_{RF} - \mu_{AA} > 0$, where AA is one of A2C, DQN or PPO

⁵What does a single data point indicate?: Consider the ‘‘Simulated’’ category – 10 training rounds \times 10 test rounds \times 3 noise settings = 300 sample points. Note that a single test round is conducted with 40 randomly sampled wear datapoints and therefore 300 samples = 300×40 i.e. 12,000 samples of wear data. Similarly, for the real-data univariate state: 3 datasets \times 10 training rounds \times 10 test rounds \times 3 noise settings = 900 sample points.

4.7 Training times

Our final set of results are related to the training time required for each algorithm. The naïve REINFORCE algorithm is extremely slow, with a very high variance in training time, as seen in Fig. 20.

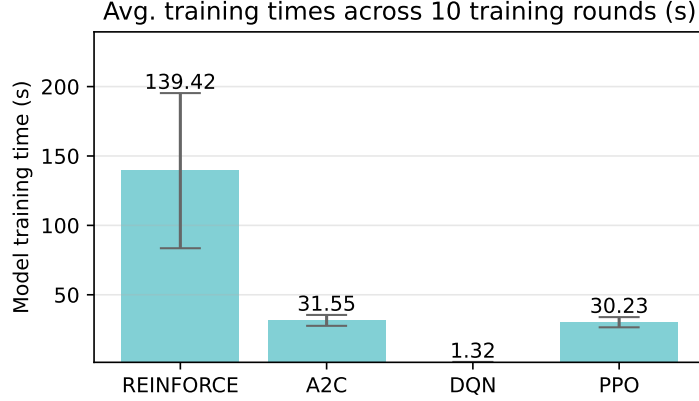


Figure 20: Training time, averaged over 10 rounds and all 15 variants.

5 Discussion

The inventor of the REINFORCE algorithm, in his original paper [Williams \(1992\)](#), mentions the inability to predict the convergent and asymptotic properties of REINFORCE algorithms using analytical means. The author mentions that *simulation studies* are the primary source of understanding its behavior. 27 years later, [Peck and Renaux \(2019\)](#) notes that rigorous convergence proofs are *not* available for many algorithms based on REINFORCE and in their paper provide an intuition for convergence properties. This supports the extensive experimental studies on REINFORCE performed by [Duan et al. \(2016\)](#); [Peck and Renaux \(2019\)](#); [Zhang et al. \(2021a,b\)](#) as well our empirical research.

Both [Duan et al. \(2016\)](#) and [Zhang et al. \(2021a\)](#) studied the behavior on multiple OpenAI Gym environments, while [Peck and Renaux \(2019\)](#) provide empirical results for MuJuCo environments. [Duan et al. \(2016\)](#) observe that, despite its simplicity it is an effective algorithm in optimizing policies based on deep neural networks. On the other hand, their empirical study concluded that REINFORCE is occasionally trapped in premature convergence to local optima. REINFORCE suffers from high variance ([Peck and Renaux, 2019](#)) and converges very slowly when it does. High variance implies that a large sample of environment interactions are needed to obtain a reasonable approximation of the actual gradient.

[Zhang et al. \(2021b\)](#) provide the first known global convergence and sample efficiency results for the REINFORCE algorithm. Their study involved controlling the number of “bad” episodes as well as applying a “doubling” trick for studying the global convergence.

Interestingly our training rounds resulted in multiple situations of “zero” performance (“bad” episodes) for REINFORCE (18 instances) as also for Stable-Baseline’s A2C implementation (12 instances); DQN and PPO did not show any occurrences.

There could be two possible reasons for the positive performance demonstrated by REINFORCE. We used ReLU (rectified linear unit) as the activation function, while the other three algorithms used hyperbolic tangent (Tanh). [Henderson et al. \(2018\)](#) studied four policy-gradient methods, including the PPO and TRPO, and observed that ReLU activation perform best. [Duan et al. \(2016\)](#) observed that *even* with a small learning rate REINFORCE sometimes resulted in large changes to policy distribution, which possibly explains the fast convergence to local optima. On the other hand we used a larger learning rate (almost 50:1) and this could have assisted in reaching global optimas when it did.

While there is no doubt that this REINFORCE naïve implementation will be unstable and occasionally produce learning patterns that are stuck in local optimas and demonstrate premature convergence, our empirical studies indicate that it did perform well for this problem and at the least deserves further research.

On the evaluation criteria: It must be noted that the classification metrics we used assume that the human preventive maintenance policy, based on experience, is ideal. In practice this might not always be the case. The RL agent is trained to replace the tool optimally i.e. maximize use before reaching the threshold wear, and replace only when necessary so as to maintain lowest possible cost of replacement. In our dataset we assume the threshold to be ideally set and base the “human” action against that, rather than a real human action, which incidentally is not available for the PHM dataset anyway.

6 Conclusion

The REINFORCE is a simple algorithm and our naïve implementation can be improved drastically, for example with the implementation of a baseline to reduce variance. We evaluated the REINFORCE along with industry grade implementations of more advanced algorithms, DQN, A2C and PPO, over 15 environment variants (simulated and real data). Despite its simplicity, known variance and convergence issues, it performed surprisingly well, as observed through numerical results, plots and statistical tests.

Implementing robust RL algorithms is complex and [Raffin et al. \(2021\)](#) mention how small implementation details can significantly impact performance that is often greater than the difference between the algorithms themselves. We hope our research will contribute to empirical evidence in the study of REINFORCE and therefore contribute in an infinitesimal way to enable AutoML for the field of predictive maintenance using RL.

Appendix A Detailed results

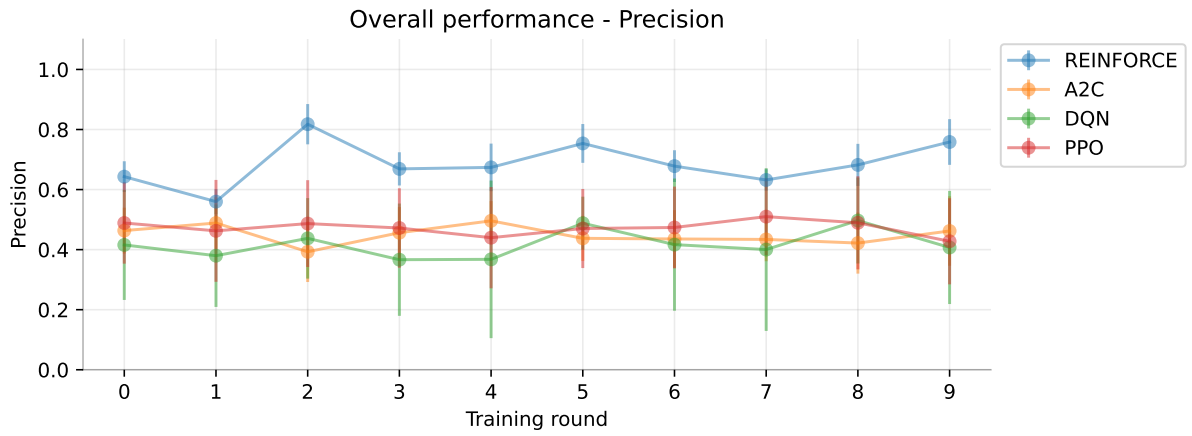
The Appendix contains detailed tabulated results as well as validation plots.

Environment	REINFORCE				A2C				DQN				PPO			
	Prec.	Recall	F1	$F_{\beta}0.5$	Prec.	Recall	F1	$F_{\beta}0.5$	Prec.	Recall	F1	$F_{\beta}0.5$	Prec.	Recall	F1	$F_{\beta}0.5$
Simulated - No noise	0.842	0.878	0.838	0.834	0.424	0.451	0.423	0.421	0.426	0.674	0.471	0.410	0.504	0.200	0.271	0.360
Simulated - Low noise	0.777	0.929	0.834	0.796	0.465	0.423	0.409	0.427	0.421	0.338	0.270	0.283	0.482	0.236	0.296	0.369
Simulated - High noise	0.798	0.940	0.851	0.816	0.358	0.281	0.256	0.272	0.447	0.519	0.380	0.360	0.514	0.207	0.286	0.382
PHM C01 SS - No noise	0.478	0.363	0.400	0.439	0.501	0.500	0.493	0.496	0.472	0.807	0.568	0.490	0.440	0.417	0.387	0.395
PHM C01 SS - Low noise	0.507	0.311	0.332	0.383	0.503	0.598	0.535	0.513	0.393	0.502	0.351	0.317	0.522	0.338	0.388	0.448
PHM C01 SS - High noise	0.693	0.562	0.579	0.623	0.266	0.282	0.267	0.262	0.458	0.525	0.400	0.384	0.456	0.369	0.372	0.400
PHM C04 SS - No noise	0.751	0.878	0.784	0.757	0.487	0.442	0.449	0.463	0.439	0.684	0.472	0.411	0.500	0.510	0.469	0.473
PHM C04 SS - Low noise	0.662	0.756	0.672	0.657	0.409	0.455	0.428	0.416	0.411	0.500	0.370	0.341	0.488	0.280	0.324	0.386
PHM C04 SS - High noise	0.611	0.713	0.620	0.598	0.518	0.607	0.552	0.530	0.358	0.451	0.325	0.294	0.428	0.262	0.286	0.333
PHM C06 SS - No noise	0.830	0.726	0.754	0.792	0.517	0.509	0.507	0.511	0.360	0.309	0.256	0.258	0.409	0.248	0.275	0.321
PHM C06 SS - Low noise	0.205	0.279	0.228	0.212	0.510	0.577	0.530	0.516	0.434	0.266	0.266	0.296	0.417	0.181	0.232	0.294
PHM C06 SS - High noise	0.709	0.843	0.759	0.726	0.316	0.324	0.311	0.308	0.449	0.518	0.400	0.375	0.388	0.222	0.265	0.317
PHM C01 MS - No noise	0.835	0.652	0.656	0.716	0.461	0.444	0.397	0.404	0.384	0.558	0.393	0.348	0.513	0.383	0.416	0.460
PHM C04 MS - No noise	0.739	0.255	0.359	0.494	0.498	0.589	0.490	0.470	0.323	0.209	0.160	0.168	0.499	0.393	0.421	0.457
PHM C06 MS - No noise	0.864	0.356	0.469	0.616	0.501	0.713	0.578	0.527	0.489	0.705	0.529	0.479	0.523	0.488	0.485	0.498

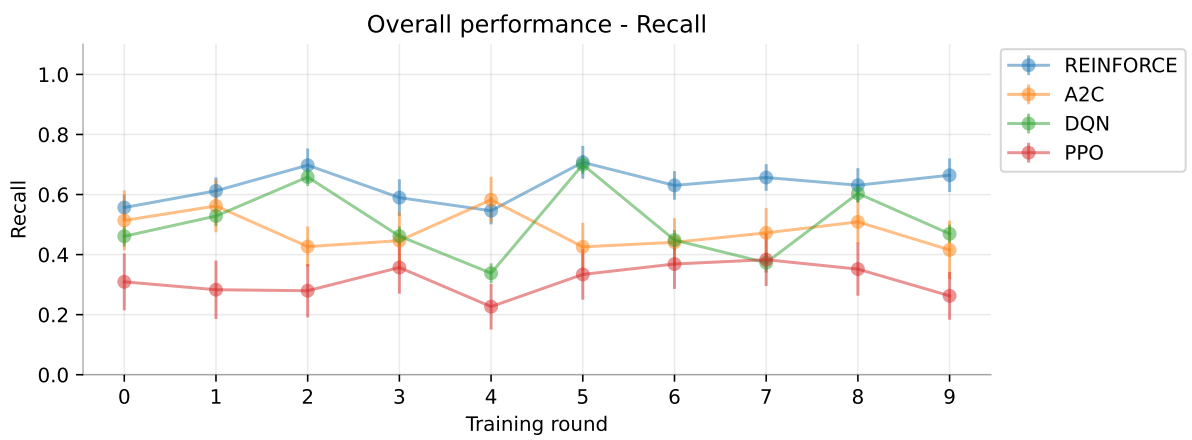
Table 10: Model performance comparison all variants of the environments, over 10 rounds of training. Maximum values indicated in blue.

Environment	REINFORCE				A2C				DQN				PPO			
	Prec.	Recall	F1	$F_{\beta}0.5$	Prec.	Recall	F1	$F_{\beta}0.5$	Prec.	Recall	F1	$F_{\beta}0.5$	Prec.	Recall	F1	$F_{\beta}0.5$
Simulated - No noise	0.897	0.960	0.926	0.908	0.500	1.000	0.667	0.556	0.505	0.980	0.667	0.560	0.669	0.430	0.518	0.597
Simulated - Low noise	0.960	0.945	0.952	0.957	0.516	1.000	0.680	0.571	0.500	0.980	0.662	0.554	0.633	0.460	0.530	0.586
Simulated - High noise	0.922	0.990	0.955	0.935	0.503	1.000	0.669	0.558	0.504	0.990	0.668	0.559	0.569	0.355	0.434	0.505
PHM C01 SS - No noise	0.889	0.995	0.939	0.908	0.586	0.625	0.603	0.592	0.647	0.970	0.776	0.693	0.543	1.000	0.703	0.597
PHM C01 SS - Low noise	0.988	0.765	0.861	0.932	0.499	0.995	0.664	0.554	0.504	0.990	0.668	0.559	0.623	0.740	0.675	0.643
PHM C01 SS - High noise	0.850	0.970	0.905	0.871	0.521	0.680	0.588	0.546	0.505	0.985	0.668	0.560	0.520	0.725	0.604	0.551
PHM C04 SS - No noise	0.811	1.000	0.895	0.842	0.536	0.645	0.583	0.554	0.501	0.965	0.660	0.554	0.579	0.895	0.702	0.622
PHM C04 SS - Low noise	0.798	0.980	0.879	0.829	0.556	0.665	0.603	0.573	0.734	0.990	0.843	0.774	0.546	0.660	0.596	0.565
PHM C04 SS - High noise	0.708	0.840	0.767	0.730	0.521	0.835	0.641	0.563	0.511	0.985	0.672	0.565	0.517	0.820	0.633	0.558
PHM C06 SS - No noise	1.000	0.895	0.944	0.977	0.520	0.680	0.587	0.545	0.935	0.975	0.954	0.942	0.587	0.650	0.615	0.597
PHM C06 SS - Low noise	0.943	0.795	0.861	0.908	0.501	1.000	0.668	0.557	0.961	0.725	0.826	0.901	0.552	0.370	0.438	0.497
PHM C06 SS - High noise	0.821	0.845	0.831	0.825	0.540	0.755	0.628	0.572	0.980	0.960	0.969	0.976	0.521	0.615	0.564	0.537
PHM C01 MS - No noise	0.827	0.995	0.903	0.856	0.500	1.000	0.667	0.556	0.505	0.985	0.668	0.560	0.512	0.595	0.549	0.526
PHM C04 MS - No noise	0.910	0.425	0.577	0.738	0.500	1.000	0.667	0.556	0.501	0.975	0.662	0.555	0.501	0.635	0.558	0.522
PHM C06 MS - No noise	0.934	0.865	0.896	0.918	0.500	1.000	0.667	0.556	0.969	0.600	0.741	0.863	0.497	0.690	0.577	0.526

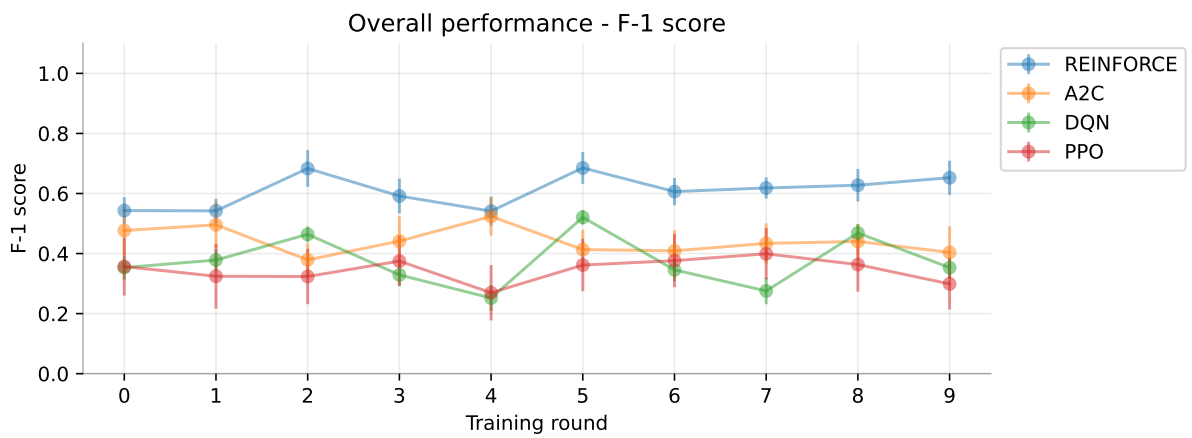
Table 11: Super Models: Best models selected over 10 rounds of training. Maximum performance values indicated in blue.



(a) Precision

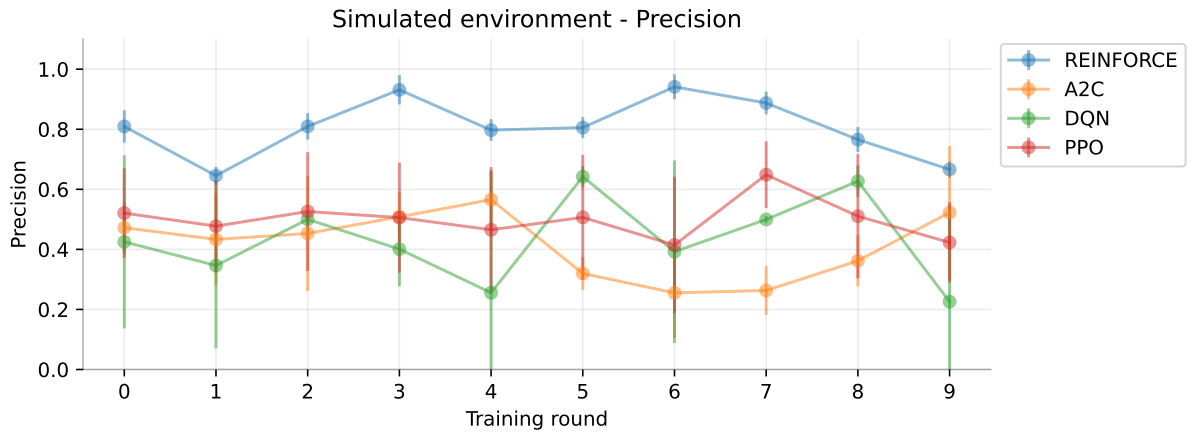


(b) Recall

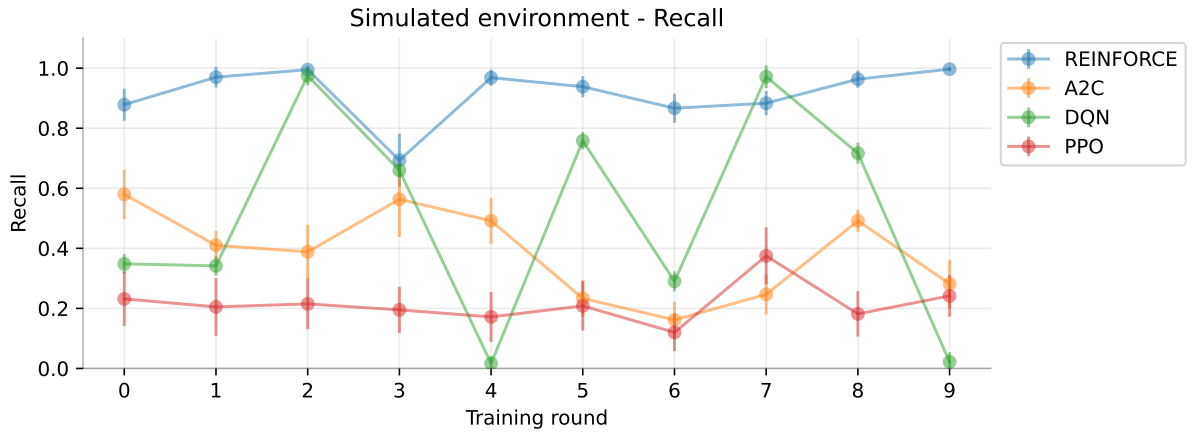


(c) F1-score

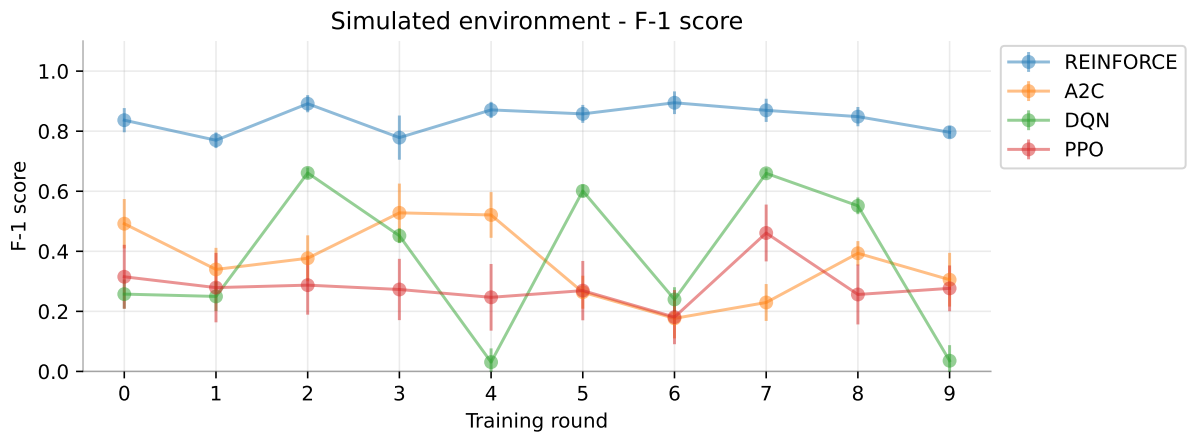
Figure 21: Overall performance – Average over 10 models



(a) Precision

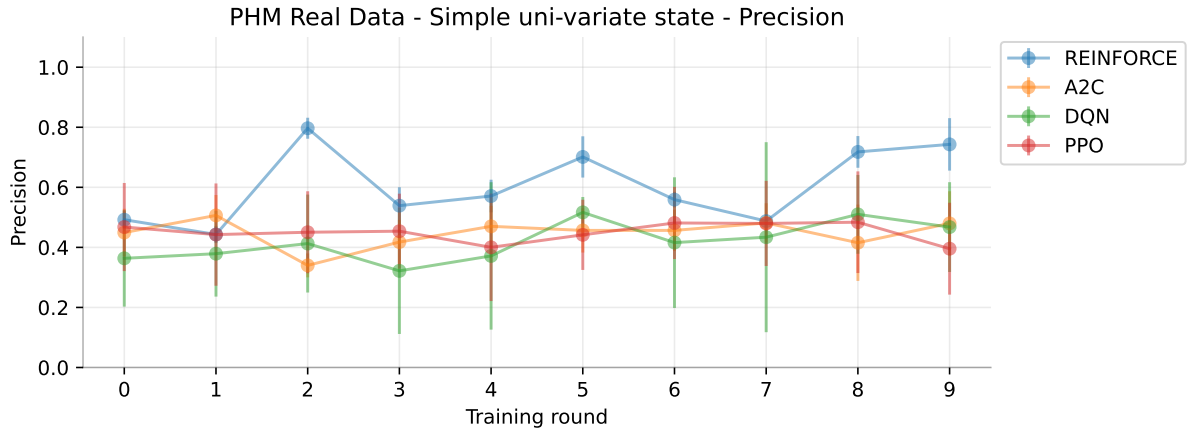


(b) Recall

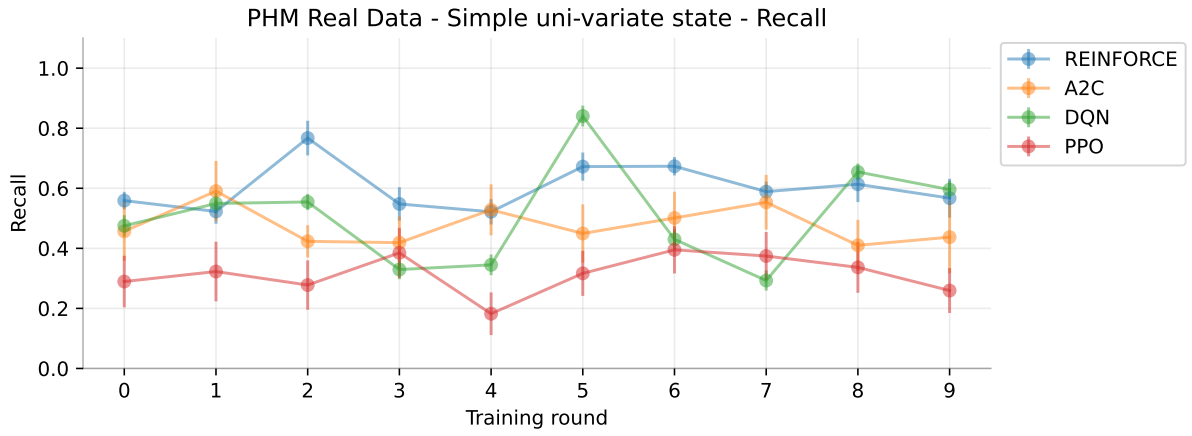


(c) F1-score

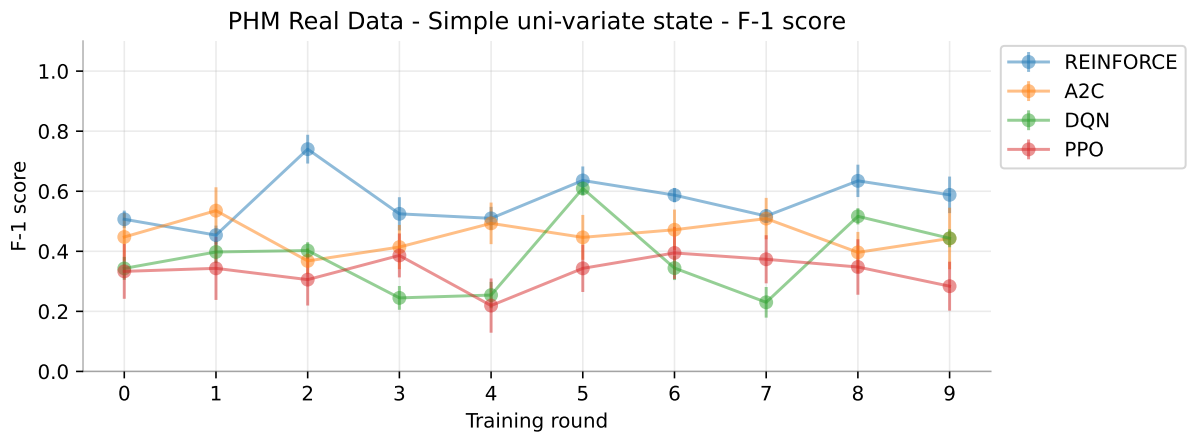
Figure 22: Simulated environment – Average over 10 models



(a) Precision

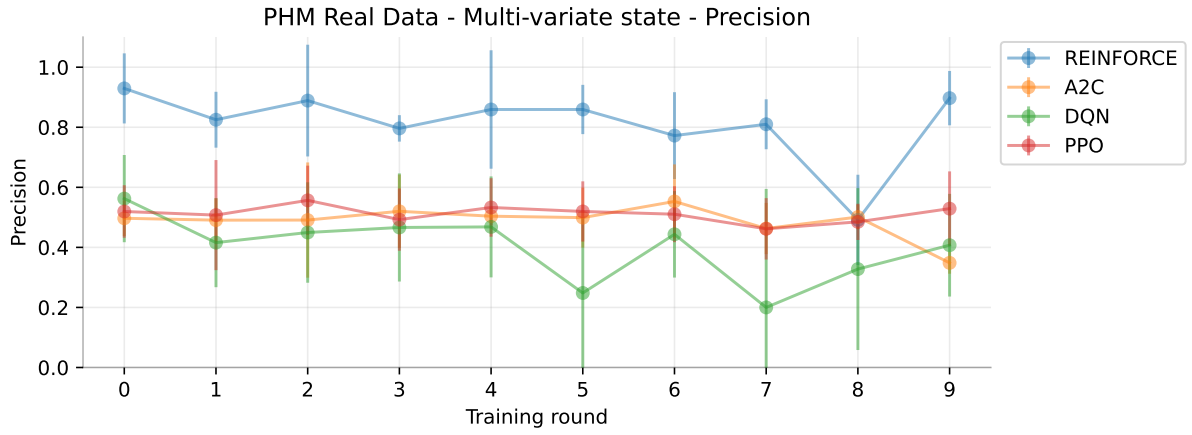


(b) Recall



(c) F1-score

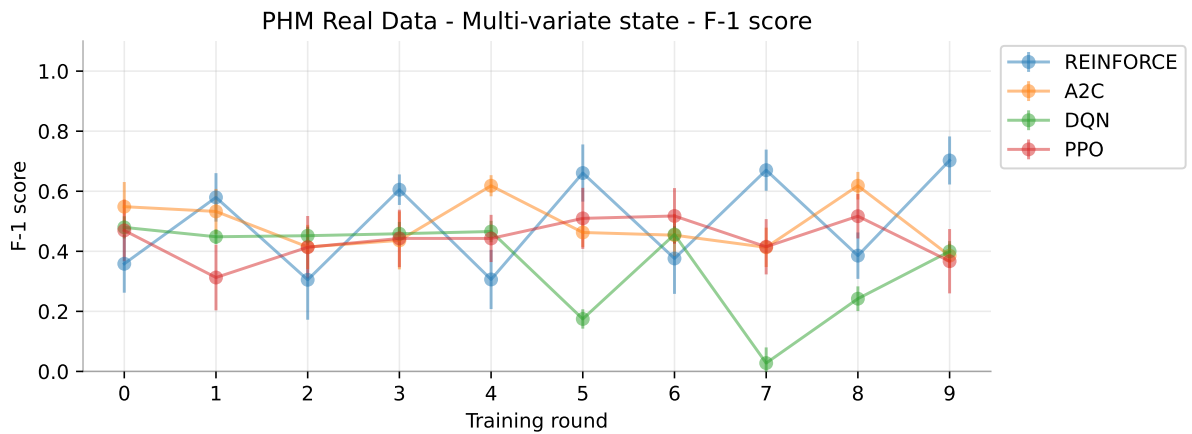
Figure 23: Univariate state environment – Average over 10 models



(a) Precision



(b) Recall



(c) F1-score

Figure 24: Multivariate state environment – Average over 10 models

References

- Predrag Dašić. Analysis of wear cutting tools by complex power-exponential function for finishing turning of the hardened steel 20crmo5 by mixed ceramic tools. *Fascicle VIII Tribology*, 12:54–60, 2006.
- Yan Duan, Xi Chen, Rein Houthooft, John Schulman, and Pieter Abbeel. Benchmarking deep reinforcement learning for continuous control. In *International conference on machine learning*, pages 1329–1338. PMLR, 2016.
- Gabriel Dulac-Arnold, Nir Levine, Daniel J Mankowitz, Jerry Li, Cosmin Paduraru, Sven Gowal, and Todd Hester. An empirical investigation of the challenges of real-world reinforcement learning. *arXiv preprint arXiv:2003.11881*, 2020.
- Gabriel Dulac-Arnold, Nir Levine, Daniel J Mankowitz, Jerry Li, Cosmin Paduraru, Sven Gowal, and Todd Hester. Challenges of real-world reinforcement learning: definitions, benchmarks and analysis. *Machine Learning*, 110(9):2419–2468, 2021.
- L. Erhan, M. Ndubuaku, M. Di Mauro, W. Song, M. Chen, G. Fortino, O. Bagdasar, and A. Liotta. Smart anomaly detection in sensor systems: A multi-perspective review. *Information Fusion*, 67:64–79, 2021. doi: 10.1016/j.inffus.2020.10.001.
- SA Ford and M Ritchie. Cognitive radar mode control: a comparison of different reinforcement learning algorithms. In *International Conference on Radar Systems (RADAR 2022)*, volume 2022, pages 107–112. IET, 2022.
- Future Market Insights. Milling machine market outlook (2023 to 2033), 1 2023. URL <https://www.futuremarketinsights.com/reports/milling-machine-market>. Accessed: 2023-06-23.
- Peter Henderson, Riashat Islam, Philip Bachman, Joelle Pineau, Doina Precup, and David Meger. Deep reinforcement learning that matters. In *Proceedings of the AAAI conference on artificial intelligence*, volume 32, 2018.
- Xinghui Li. 2010 phm society conference data challenge, 2021. URL <https://dx.doi.org/10.21227/jdxd-yy51>.
- Volodymyr Mnih, Koray Kavukcuoglu, David Silver, Alex Graves, Ioannis Antonoglou, Daan Wierstra, and Martin Riedmiller. Playing atari with deep reinforcement learning. *arXiv preprint arXiv:1312.5602*, 2013.
- Volodymyr Mnih, Adria Puigdomenech Badia, Mehdi Mirza, Alex Graves, Timothy Lillicrap, Tim Harley, David Silver, and Koray Kavukcuoglu. Asynchronous methods for deep reinforcement learning. In *International conference on machine learning*, pages 1928–1937. PMLR, 2016.
- Marcel Panzer and Benedict Bender. Deep reinforcement learning in production systems: a systematic literature review. *International Journal of Production Research*, 2021.
- Ryan Peck and Louis Renaux. A review of reinforce algorithms. 2019.

- Antonin Raffin, Ashley Hill, Adam Gleave, Anssi Kanervisto, Maximilian Ernestus, and Noah Dormann. Stable-baselines3: Reliable reinforcement learning implementations. *J. Mach. Learn. Res.*, 22(1), jan 2021. ISSN 1532-4435.
- N Sandeep Varma, Vaishnavi Sinha, and K Pradyumna Rahul. Experimental evaluation of reinforcement learning algorithms. In *International Conference on Computational Intelligence and Data Engineering*, pages 469–484. Springer, 2022.
- SB3-Algorithms. Stable-baselines3 - master list of algorithms, 2022. URL <https://stable-baselines3.readthedocs.io/en/master/guide/algos.html>. Accessed: 2023-06-27.
- SB3-Default Network Architecture. Stable-baselines3 - default network architecture, 2022. URL https://stable-baselines3.readthedocs.io/en/master/guide/custom_policy.html#default-network-architecture. Accessed: 2023-06-27.
- John Schulman, Sergey Levine, Pieter Abbeel, Michael Jordan, and Philipp Moritz. Trust region policy optimization. In *International conference on machine learning*, pages 1889–1897. PMLR, 2015.
- John Schulman, Filip Wolski, Prafulla Dhariwal, Alec Radford, and Oleg Klimov. Proximal policy optimization algorithms. *arXiv preprint arXiv:1707.06347*, 2017.
- Rajesh Siraskar, Satish Kumar, Shruti Patil, Arunkumar Bongale, and Ketan Kotecha. Reinforcement learning for predictive maintenance: a systematic technical review. *Artificial Intelligence Review*, pages 1–63, 2023.
- Richard Sutton and Andrew Barto. *Reinforcement Learning: An Introduction*. The MIT Press, Cambridge, England, 2nd. edition edition, 2018.
- Krishna Velivela and Sudhir Yarram. Comparison of reinforcement learning algorithms, Dec 2020.
- Ronald J Williams. Simple statistical gradient-following algorithms for connectionist reinforcement learning. *Reinforcement learning*, pages 5–32, 1992.
- Junyu Zhang, Chengzhuo Ni, Csaba Szepesvari, Mengdi Wang, et al. On the convergence and sample efficiency of variance-reduced policy gradient method. *Advances in Neural Information Processing Systems*, 34:2228–2240, 2021a.
- Junzi Zhang, Jongho Kim, Brendan O’Donoghue, and Stephen Boyd. Sample efficient reinforcement learning with reinforce. In *Proceedings of the AAAI conference on artificial intelligence*, volume 35, pages 10887–10895, 2021b.